Subunit III of Cytochrome *c* Oxidase Influences the Conformation of Subunits I and II: An Infrared Study†

Izaskun Echabe,‡ Tuomas Haltia,§,|| Ernesto Freire,§ Félix M. Goñi,‡ and José Luis R. Arrondo*,‡

Departamento de Bioquímica, Universidad del Pais Vasco, P.O. Box 644, E-48080 Bilbao, Spain, and Departments of Biology and Biophysics and Biocalorimetry Center, The Johns Hopkins University, Baltimore, Maryland 21218

Received May 1, 1995; Revised Manuscript Received July 11, 1995⊗

ABSTRACT: The secondary structure of wild-type *Paracoccus denitrificans* cytochrome *c* oxidase obtained by decomposition of the infrared amide I band contains 44% α-helix, 18% β-sheet, 14% β-turns, 18% loops, and 6% nonordered segments. The mutant lacking subunit III presents a small but significant increase (from 18% to 24%) in the percentage of loops and slight differences in the other components. Using band/area ratios and tyrosine side chain absorption as an inner standard, it is shown that in the absence of subunit III the structure of subunits I and II is altered although no changes in their α-helix or β-sheet content are observed. In the bacterial oxidase, thermal infrared studies show a complex denaturation pattern characterized by the presence of a partially denatured intermediate state. Of the seven predicted subunit III α-helices, only four are resistant toward the thermal challenge and behave as expected for typical transmembrane helices. The observation that the absence of subunit III influences the conformation of loop regions in the two other subunits suggests that part of the interaction surface between subunit III and the catalytic subunits might be located outside the lipid bilayer.

Respiratory cytochrome *c* oxidases are membrane proteins that reduce dioxygen into water. They are found in all three domains of life: eukaryotes, eubacteria, and archaea (Castresana *et al.,* 1994; Garcia-Horsman *et al.,* 1994). The subclass of aa_3-type cytochrome *c* oxidases has three homologous core polypeptides called subunits I, II, and III (Brown *et al.,* 1993). These subunits have been predicted to contain a total of 21 transmembrane helices (Saraste, 1990); the view has been supported by gene fusion experiments with individual subunits (Chepuri & Gennis, 1990). The active site of the enzyme, a spin-coupled heme−copper centre, is located in subunit I, which is thought to contain 12 transmembrane segments. This subunit also houses the low-spin heme which is the electron donor to the active site. Subunit II has only two transmembrane spans, and most of it is situated on the periplasmic side of the bacterial cell membrane (Lappalainen *et al.,* 1993). It is the latter, largely β-sheet domain which carries the electron entry site of the enzyme, the Cu_A-site (Hill, 1993).

In contrast to subunits I and II, no well-defined role has been assigned for subunit III, which has no redox-active groups. Subunit III is often depicted as having seven transmembrane spans (Saraste, 1990). It appears to interact relatively weakly with the entity made up of subunits I and II. Active two-polypeptide oxidases have been isolated from *Paracoccus denitrificans* either by depletion of subunit III or from a mutant devoid of subunit III gene (Hendler *et al.,* 1991; Haltia *et al.,* 1994). However, in the absence of subunit III, the membrane-bound oxidase is partially inactive and heterogeneous (Haltia *et al.,* 1989). Two point mutations in subunit III have been reported to be linked to a pathologic condition (Johns & Neufeld, 1993). Recent results indicate that subunit III has an effect on the oxygen reducing site in subunit I (Haltia *et al.,* 1994).

Infrared spectroscopy (IR) has been previously used to characterize cytochrome *c* oxidases. The infrared amide I band, arising mainly from C=O stretching vibrations of the peptide bond, is conformationally sensitive and can be decomposed into its component bands in order to obtain additional structural information (Arrondo *et al.,* 1993). A combination of structural analysis and thermal denaturation studies has revealed tertiary structure differences between mitochondrial cytochrome *c* oxidase in solution and in a crystalline array (Arrondo *et al.,* 1994). Also, infrared spectroscopy has been used to characterize interactions between the polypeptide and the heme centers (Hosler *et al.,* 1994). We have shown recently, using differential scanning calorimetry (DSC) (Haltia *et al.,* 1994), that the thermal denaturation profile of *P. denitrificans* wild-type cytochrome *c* oxidase ($pCOX_{wt}$) is composed of two separate transitions, caused by subunit III and by subunits I and II together at low and high temperatures, respectively [see Figure 3 of Haltia *et al.* (1994)]. The two-subunit mutant preparation ($pCOX_{III}-$) exhibits only the high-temperature transition. In this study, we use infrared spectroscopy to investigate the structure and thermal profile of both bacterial oxidases. The combined results obtained from spectra of wild-type and mutant enzymes provide information on the secondary structure of the oxidase and in particular on that of subunit III and the influence of the latter on the conformation of subunits I and II.

† I.E. is supported by a predoctoral fellowship from the Basque Government. J.L.R.A. and F.M.G. have been supported by Grant 161/92 from the Universidad del Pais Vasco and Grant PB91-0441 from DGICYT. T.H. acknowledges a grant from the Magnus Ehrnrooth Foundation. E.F. is supported by grants from the National Institutes of Health (RR04328 and GM37911).

* Corresponding author. Phone: +34-4-464-7700, x2407. Fax: +34-4-464-8500. E-mail: GBPROARJ@LG.EHU.ES.

‡ Universidad del Pais Vasco.

§ The Johns Hopkins University.

|| Present address: Institute of Biomedicine, Department of Medical Chemistry, University of Helsinki, P.O. Box 8, FIN-00014, Finland.

⊗ Abstract published in *Advance ACS Abstracts,* September 15, 1995.

0006-2960/95/0434-13565$09.00/0

MATERIALS AND METHODS

Paracoccus denitrificans growth, membrane preparations, and enzyme purification have been performed as recently described in Haltia *et al.* (1994).

Infrared Spectroscopy. Samples for infrared spectroscopy were prepared as described previously (Haltia *et al.*, 1994). The protein, at a concentration of ≈7 mg/mL for the mutant and ≈20 mg/mL for the wild-type strain, was placed in a thermostated cell with CaF_2 windows. Path lengths were 6 μm for the H_2O experiments and 50 μm for the D_2O measurements, unless otherwise stated. Spectra were acquired in a Nicolet Magna 550 spectrometer equipped with an MCT detector. Typically, 1000 scans for each, background and sample, were collected and the spectra obtained with a nominal resolution of 2 cm^{-1} and points encoded at 1 cm^{-1}. Data treatment and band decomposition of the original amide I have been described elsewhere (Castresana *et al.*, 1988; Arrondo *et al.*, 1989, 1993, 1994; Bañuelos *et al.*, 1995). Briefly, for each component four parameters are considered: band position, band height, bandwidth, and bandshape. Thus, in a typical amide I band decomposition with 6 or 7 band components, the number of parameters is 24−28. The number and position of component bands are obtained through deconvolution and derivation; initial heights are set at 90% of those in the original spectrum for the bands in the wings and for the most intense component and at 70% of the original intensity for the other bands. Initial bandwidths are estimated from the Fourier derivative. The Lorentzian component of the bands is initially set at 10%. The base line is removed prior to starting the fitting process. The iteration procedure is carried out in two steps as described (Bañuelos *et al.*, 1995). The mathematical solution to the decomposition may not be unique, but if restrictions are imposed such as the maintenance of the initial band positions in an interval of ±1 cm^{-1}, the preservation of the bandwidth within the expected limits, or the agreement with theoretical boundaries or predictions, the result becomes, in practice, unique. The results are verified by constructing artificial curves with the parameters obtained and performing the band decomposition on those, with identical outcome. The methodology has also been checked with well-characterized proteins e.g., myoglobin or concanavalin A.

Thermal Treatments. Thermal studies were carried out either by a step-heating method with ≈3 °C steps, leaving the sample to stabilize for 5 min at each step before recording the corresponding spectra, or by a continuous heating method. This method uses the Series and Rapid Scan software from OMNIC (Nicolet Corp., Madison, WI). A total of 164 interferograms/min, using 100 μm path length, are collected at 2 cm^{-1} resolution and averaged after each minute. The sample is heated in the interval 20−80 °C at 1 °C/min. Hence, each interferogram corresponds roughly to 1 °C. Temperature is monitored by a probe situated at the edge of the window. After spectral recording, the interferograms are processed by ratioing with respect to a background, and spectra are obtained as in the step-heating method. A drawback of the continuous heating method is that the number of spectra averaged for each point is comparatively low. In D_2O, the problem is avoided in part by increasing the path length from 50 to 100 μm, but this is not possible in H_2O, because the path length has to be kept at 6 μm in order to prevent excessive H_2O absorption. The maximum number of spectra that can be acquired in H_2O (304 at 4 cm^{-1}) does not produce a signal-to-noise ratio good enough to perform the above mathematical procedures with precision. Therefore, continuous heating spectra are shown only in D_2O. Reducing the resolution from 2 to 4 cm^{-1} would also increase the signal-to-noise ratio, but our previous work on cytochrome oxidase was made with a nominal resolution of 2 cm^{-1}, that has been maintained in the present study.

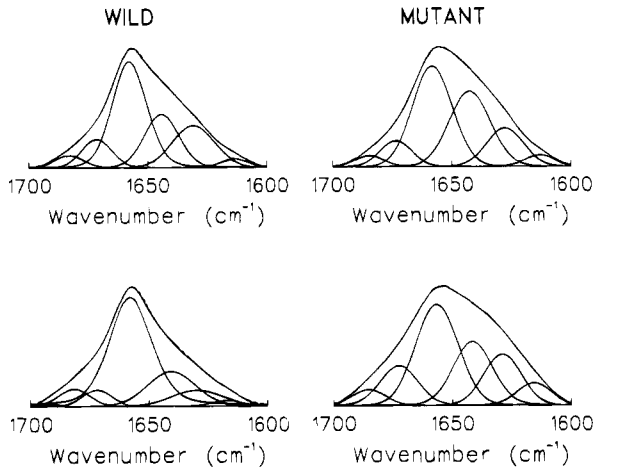

FIGURE 1: Amide I band decomposition of the wild-type (left) and the mutant lacking subunit III (right) cytochrome *c* oxidase from *P. denitrificans* in a H_2O (lower traces) or a D_2O (upper traces) medium. Contour: experimental, continuous line; reconstructed by addition of band components, dashed line.

Table 1: Values Corresponding to Band Position and Percentage Area Obtained after Decomposition of the Amide I Band of *Paracoccus denitrificans* Cytochrome *c* Oxidase[a]

wild				mutant			
H_2O		D_2O		H_2O		D_2O	
band position	% area	band position	% area	band position	% area	band position	% area
1691	<1			1692	<1		
1682	3	1686	3	1681	6	1685	3
1672	11	1674	10	1672	7	1673	9
1658	50	1658	44	1658	47	1658	42
1643	18	1644	24	1642	24	1643	32
1630	17	1630	18	1629	16	1628	15

[a] The values are rounded off to the nearest integer.

RESULTS

Structure of P. denitrificans Cytochrome c Oxidase. The solution structure of wild-type cytochrome *c* oxidase from *P. denitrificans* ($pCOX_{wt}$) and of a mutant lacking subunit III ($pCOX_{III}-$) has been obtained from the conformationally-sensitive infrared spectral bands arising from the peptide bond (Arrondo *et al.*, 1993). The most important band in conformational studies is the amide I band which is located between 1700 and 1600 cm^{-1}, and is due mainly (≈80%) to the carbonyl stretching vibration of the peptide bond. Decomposition of the original amide I band in H_2O and D_2O media into its constituents improves the assignment of the component bands to specific structural features (Arrondo *et al.*, 1994). Figure 1 displays the decomposed band contours of $pCOX_{wt}$ and $pCOX_{III}-$ in both media, and the parameters obtained are shown in Table 1. Six components attributable to protein conformations are seen in the H_2O spectrum, and five in D_2O. The component at around 1690 cm^{-1} in the

Table 2: Secondary Structure of Wild Type and a Mutant Lacking Subunit III from *Paracoccus denitrificans* Cytochrome *c* Oxidase[a]

	wild type	mutant
α-helix	44	41
β-sheet	18	17
β-turns	14	13
unordered	6	5
loops	18	24

[a] The values are obtained from Table 1 according to the procedure of Arrondo *et al.* (1994)

Table 3: Area Ratios of Band Components of the Cytochrome *c* Oxidase Amide I Band, and the Normalized Area of the C−C Tyr Ring Vibration at 1515 cm^{-1}

band area ratio[b]	assignment	wild	mutant
1658/1644	α/loops+unordered	2.03	1.15
1658/1630	α/β	2.18	2.15
1630/1644	β/loops+unordered	0.93	0.53
1658/1670+1680	α/turns	3.8	2.8
1658/Tyr	α	1.99	2.08
1644/Tyr	loops+unordered	1.07	1.88
1630/Tyr	β	0.93	0.95
1670+1680/Tyr	turns	0.58	0.72

[a] Spectra taken in D_2O buffer. [b] Band positions are approximate, since they differ slightly between the wild type and mutant enzyme.

H_2O spectra, due to the high-frequency band of the antiparallel β-sheet, shifts to around 1675 cm^{-1} in a D_2O medium. As expected from theoretical studies, this band is weak as compared to its low-frequency counterpart located at around 1630 cm^{-1}. The assignment of the bands has been described previously (Arrondo *et al.*, 1994), and no unusual components are present in these proteins. The secondary structure of $pCOX_{wt}$ and $pCOX_{III}-$ as obtained from the combined values in H_2O and D_2O media is shown in Table 2. Interpretations of the differences between the wild-type and mutant proteins based on percentage changes are difficult because of the different number of amino acids involved in each protein. Hence, parameters less affected by multiple alterations must be used in order to obtain information on the changes produced in individual components. Band area ratios (Table 3) isolate two components and make them comparable between both samples. The ratio α-helix/β-sheet (1658/1630) is constant in $pCOX_{wt}$ and $pCOX_{III}-$, implying that these two conformations do not vary in relation to each other when subunit III is not present. However, differences are seen in the ratios involving loops, unordered structure, or β-turns. To ensure that a constant band ratio does not arise from a simultaneous change in the two bands involved, absolute areas can be ratioed to an internal reference (a nonconformational band, e.g., an amino acid side chain band). The tyrosine C−C ring stretching vibration located at 1515 cm^{-1} gives rise to an isolated band in the D_2O spectrum that is useful for this purpose. Figure 2 shows the spectra of wild-type and mutant cytochrome *c* oxidase in the 1800−1500 cm^{-1} region in which the tyrosine band and the amide I components are shown. The ratio of component area *vs* the 1515 cm^{-1} band area (normalized to the number of tyrosines, 46 in the wild-type enzyme and 36 in the mutant) is shown in Table 3. It can be seen that whereas the bands at around 1658 and 1630 cm^{-1}, related to α-helix and β-sheet, keep a constant ratio, the band around 1640 cm^{-1}, related to loops and unordered conformation, changes considerably. A smaller increase is observed in the value

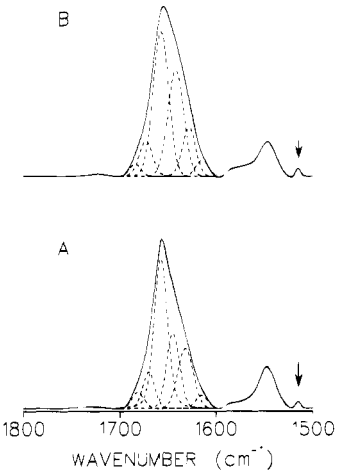

FIGURE 2: The 1800−1500 cm^{-1} region of the wild-type (A) and mutant (B) cytochrome *c* oxidases from *P. denitrificans* showing the amide I band and the tyrosine C−C ring stretching band (arrow). Both have been fitted to their components; in the latter case, the single-component fitting overlaps the band contour. The spectra have been base-line-corrected using a spline curve.

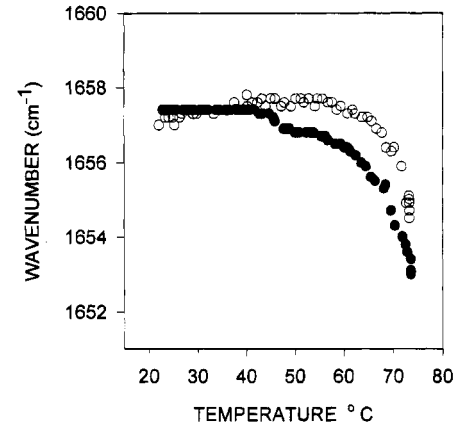

FIGURE 3: Plot of band position vs temperature of the component corresponding to α-helix for wild (●) and mutant (○) *P. denitrificans* cytochrome *c* oxidase.

of the 1670 + 1680 cm^{-1} bands, related to β-turns. Thus, we conclude that the α-helix and β-sheet structures are preserved in the mutant in the absence of subunit III, whereas unordered structure, loops, and β-turns are affected by the loss of this subunit.

Thermal Denaturation of P. denitrificans Cytochrome c Oxidase. Differential scanning calorimetry and infrared studies have shown that the thermal denaturation of $pCOX_{wt}$ is a complex process (Haltia *et al.*, 1994). Two transitions centered at 48 and 68 °C were observed in calorimetric studies, while in $pCOX_{III}-$ the transition at 48 °C was not detected. However, the corresponding transition temperatures were lower in the infrared data due to the slower heating rate used in the infrared experiments. The infrared thermal study of $pCOX_{wt}$ has now been performed matching the DSC studies by using a constant heating rate of 1 °C/min (see Materials and Methods). Figure 3 shows the temperature dependence of the band position of the α-helix (1658 cm^{-1}) component in a D_2O buffer. In agreement with the earlier DSC results, two transitions are seen centered around 47 and 67 °C, the temperatures obtained by DSC, that define three conformational states in $pCOX_{wt}$. These transition temperatures depend on the heating rate (as expected for a kinetically controlled process): at a heating rate of, e.g., 0.5

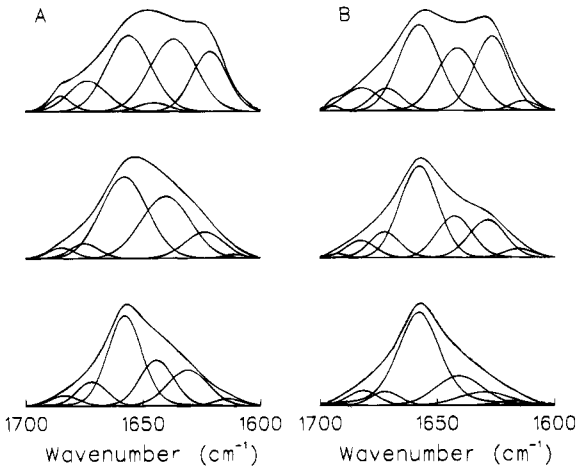

FIGURE 4: Amide I band decomposition of wild cytochrome *c* oxidase in D_2O (A) and H_2O (B) media at room temperature (lower traces), in the intermediate state (medium traces), and after thermal denaturation (upper traces). Contour: experimental, continuous line; reconstructed by addition of band components, dashed line.

Table 4: Secondary Structure of Wild-Type Cytochrome *c* Oxidase from *Paracoccus denitrificans* at Low Temperature (≈20 °C), in the Intermediate State (≈55 °C), and after Thermal Denaturation (≈70 °C)

structure	low	intermediate	high
α-helix	44	36	30 + 14
extended chains[a]	18	17	18 + 10
β-turns	14	15	16
unordered	6	16	2
loops	18	16	10

[a] Including β-sheet.

°C/min, the temperatures are 44 and 63 °C (not shown). The event defined by the two transition temperatures may not be purely conformational, since a change in band shape could be produced by a partial H → D exchange. To exclude this possibility, the study was also performed in H_2O medium (Arrondo *et al.*, 1994). As stated under Materials and Methods, measurements in H_2O cannot be made using a constant heating rate, because the signal-to-noise ratio obtained is not good enough for the quantitative analysis. However, even if the temperatures defining the intermediate state are affected by the method used, the conformation of the three different cases is the same irrespective of the heating routine. Figure 4 shows the decomposed amide I in D_2O and H_2O corresponding to each of the three states, and the respective conformational data are presented in Table 4. The main effect of heating from room temperature to the intermediate state is an increase in the unordered structure with a decrease in the α-helix conformation. The denatured protein in turn shows an important increase in the bands due to intermolecular contacts, characteristic of aggregation associated with irreversible protein denaturation, and a rearrangement of the other structures. Assignment of the bands after thermal denaturation is difficult, because of the presence of distorted structures. As an example, the band at 1648 cm^{-1} in D_2O has been attributed to distorted α-helices (Naumann *et al.*, 1993). In fact, the sum of this band and the one corresponding to unaltered α-helix (≈1658 cm^{-1}) equals the value for α-helix contribution at room temperature. The extended structures are more difficult to define due to structural rearrangements. In H_2O, only a band at 1626 cm^{-1} is obtained, whereas in D_2O two bands emerge, at 1621 and 1635 cm^{-1}, related to extended structures. The β-sheet structure observed in the denatured protein is predictably not the same than at room temperature, because of the observed shifts in position from 1630 to 1635 cm^{-1}.

In $pCOX_{III}-$, the low-temperature conformational change is not seen and, in agreement with the DSC results (Haltia *et al.*, 1994), only a high-temperature event is observed.

DISCUSSION

Infrared spectroscopic studies of *P. denitrificans* cytochrome *c* oxidase have been carried out to elucidate the secondary structure and the role of subunit III in maintaining the structure of the enzyme. The number of amino acids of the different subunits of cytochrome *c* oxidase from *P. denitrificans* is 558 for subunit I, 252 for subunit II, 273 for subunit III, and about 60 for the subunit IV found in our preparations (Haltia *et al.*, 1994), making up a total of 1143 amino acids. Subunits III and IV are not present in the mutant, and the number of amino acids is in that case 810. The α-helix content of $pCOX_{wt}$ is 44%, and that of $pCOX_{III}-$ is 41%, involving 503 and 332 amino acids, respectively, in the putative helical segments. It has been suggested that subunit I has 12 transmembrane segments including 264 amino acids and that subunit II has 2 transmembrane segments with 45 amino acids (Saraste, 1990; Garcia-Horsman *et al.*, 1994; Brown *et al.*, 1993). If those predictions and our interpretation of the IR data that the α-helical segments are preserved in the mutant are correct, then there would be an excess ≈25 amino acids involved in nontransmembrane helical segment(s) in subunits I and II.

The above percentages are average values from band decompositions of different spectra, and some variation is produced by the spectral noise (Arrondo *et al.*, 1994). The interval corresponding to the 332 average figure given above is 322−345, which could only account for small changes in the length of the putative extramembranous helical segment or imply some extra amino acids in the predicted intramembrane helices.

In $pCOX_{wt}$, the excess α-helix amino acids when compared with $pCOX_{III}-$ is 171, which agrees with the prediction of 7 α-helical segments for subunit III (Saraste, 1990). The β-sheet structure involves 207 amino acids in $pCOX_{wt}$ and 138 amino acids in $pCOX_{III}-$, implying 69 amino acids involved in the β-sheet structure in subunits III and IV. The number of amino acids in extended structure in subunits I and II would then be 138. Current models for the extramembranous portion of subunit II suggest a cupredoxin fold (Van der Oost *et al.*, 1992; Garcia-Horsman *et al.*, 1994) that would account for the β-sheet structure observed by IR. Since the normalized area ratios of loops, turns, and unordered structure vary between the wild-type and mutant protein (Table 3), then an approach similar to that used with α-helix and β-sheet cannot be undertaken. Nevertheless, it can be concluded that the absence of subunit III does not affect α-helix and β-sheet, but produces changes in unordered structure, turns, and loops. Conformational differences of this type can influence heme binding or affect the oxygen reduction site: it has been shown recently (Hosler *et al.*, 1994) by various spectroscopic techniques, including infrared

spectroscopy, that a loop between transmembrane helices IX and X of subunit I caps the heme a−heme a_3−Cu_B center. The conformational changes described here are consistent with a decrease of electron transfer activity (Haltia *et al.*, 1994) and also with the preservation of proton translocation activity (Hendler *et al.*, 1991; Haltia *et al.*, 1991) by a variation in the extramembranous portion of the protein. This change can also produce effects in the intramembranous component. Interestingly, the absence of subunit III has been shown to cause slippage, i.e., uncouple electron transfer from proton translocation (Steverding *et al.*, 1993). Furthermore, it has been suggested that subunit III influences the dielectric constant in the vicinity of the heme a_3 vinyl side chain (Heibel *et al.*, 1993).

Considering the changes in loops and unordered structure in the absence of subunit III, it is tempting to suggest that these changes are localized to the extramembrane surface that is involved in the subunit III/subunit I + II interaction. The structural and functional effects observed in the absence of subunit III (see above), though involving intramembranous protein structures, may well be transmitted from the aqueous portion through the protein structure.

The thermal profile of the α-helix component defines an intermediate state in $pCOX_{wt}$ that is not present in $pCOX_{III}$− or in the bovine mitochondrial enzyme (Arrondo *et al.*, 1994) and is characterized by a 8% decrease in helical conformation (Table 4). The thermal event producing this intermediate conformation is associated only with subunit III (Haltia *et al.*, 1994). Therefore, two populations of α-helices appear to exist in subunit III, differing in their thermal response. Taking into account that secondary structure elements residing inside the lipid bilayer are extremely stable as compared to structures exposed to the aqueous milieu (Lemmon & Engelman, 1994; Haltia & Freire, 1995), the results might indicate that some of the subunit III helices have an anomalously unstable native state.

In summary, the present work deals with the secondary structure of *P. denitrificans* cytochrome *c* oxidase and with that of a mutant lacking subunit III. This study provides the first direct evidence for a role of subunit III in the structure of the oxidase. The conformation of the subunits has been determined, and the role of subunit III in the structure of the enzyme has been clarified. Most notably, the absence of subunit III appears to produce an increase in the proportion of loops in subunits I and II. The complex thermal denaturation of $pCOX_{wt}$ defines an intermediate state where a partial unfolding of subunit III α-helical segments has been demonstrated, as postulated by DSC.

ADDED IN PROOF

After acceptance of this paper, the structure at 2.8 Å resolution has been published (Iwata *et al.*, 1995) showing the interaction of subunit III loops with subunit I+II loops.

REFERENCES

Arrondo, J. L. R., Muga, A., Castresana, J., Bernabeu, C., & Goñi, F. M. (1989) *FEBS Lett. 252*, 118−120.

Arrondo, J. L. R., Muga, A., Castresana, J., & Goñi, F. M. (1993) *Prog. Biophys. Mol. Biol. 59*, 23−56.

Arrondo, J. L. R., Castresana, J., Valpuesta, J. M., & Goñi, F. M. (1994) *Biochemistry 33*, 11650−11655.

Bañuelos, S., Arrondo, J. L. R., Goñi, F. M., & Pifat, G. (1995) *J. Biol. Chem. 270*, 9192−9196.

Brown, S., Moody, A. J., Mitchell, R., & Rich, P. R. (1993) *FEBS Lett. 316*, 216−223.

Castresana, J., Muga, A., & Arrondo, J. L. R. (1988) *Biochem. Biophys. Res. Commun. 152*, 69−75.

Castresana, J., Lübben, M., Saraste, M., & Higgins, D. G. (1994) *EMBO J. 13*, 2516−2525.

Chepuri, V., & Gennis, R. B. (1990) *J. Biol. Chem. 265*, 12978−12986.

Garcia-Horsman, J. A., Barquera, B., Rumbley, J., Ma, J., & Gennis, R. B. (1994) *J. Bacteriol 176*, 5587−5600.

Haltia, T., & Freire, E. (1995) *Biochim. Biophys. Acta 1228*, 1−27.

Haltia, T., Finel, M., Harms, N., Nakari, T., Raitio, M., Wikström, M., & Saraste, M. (1989) *EMBO J. 8*, 3571−3579.

Haltia, T., Saraste, M., & Wikström, M. (1991) *EMBO J. 10*, 2015−2021.

Haltia, T., Semo, N., Arrondo, J. L. R., Goñi, F. M., & Freire, E. (1994) *Biochemistry 33*, 9731−9740.

Heibel, G. E., Hildebrandt, P., Ludwig, B., Steinrucke, P., Soulimane, T., & Buse, G. (1993) *Biochemistry 32*, 10866−10877.

Hendler, R. W., Pardhasaradhi, K., Reynafarje, B., & Ludwig, B. (1991) *Biophys. J. 60*, 415−423.

Hill, B. C. (1993) *J. Bioenerg. Biomembr. 25*, 115−120.

Hosler, J. P., Shapleigh, J., Tecklenburg, M. M. J., Thomas, J. W., Younkyoo, K., Espe, M., Fetter, J., Babcock, G. T., Alben, J. O., Gennis, R. B., & Ferguson-Miller, S. (1994) *Biochemistry 33*, 1194−1201.

Iwata, S., Ostermeier, C., Ludwig, B., & Michel, H. (1995) *Nature 376*, 660.

Johns, D. R., & Neufeld, M. J. (1993) *Biochem. Biophys. Res. Commun. 196*, 810−815.

Lappalainen, P., Aasa, R., Malmström, G., & Saraste, M. (1993) *J. Biol. Chem. 268*, 26416−26421.

Lemmon, M. A., & Engelman, D. M. (1994) *Q. Rev. Biophys. 27*, 157−218.

Naumann, D., Schultz, C., Görne-Tschelnokow, U., & Hucho, F. (1993) *Biochemistry 32*, 3162−3168.

Saraste, M. (1990) *Q. Rev. Biophys. 23*, 331−366.

Steverding, D., Köhnke, D., Ludwig, B., & Kadenbach, B. (1993) *Eur. J. Biochem. 212*, 827−831.

Van der Oost, J., Lappalainen, P., Musacchio, A., Lemieux, L., Rumbley, J., Gennis, R. B., Aasa, R., Pascher, T., Malmström, G., & Saraste, M. (1992) *EMBO J. 11*, 3209−3217.

BI951026J